Design and Optimization of Tunnel Boring Machines by Simulating the Cutting Rock Process using the Discrete Element Method

Roberto C. Medel-Morales and Salvador Botello-Rionda

Computational Sciences Department,
Centro de Investigación en Matemáticas, A.C.,
Jalisco S/N, Col. Valenciana, 36240, Guanajuato, Gto.,
Mexico

{medel, botello}@cimat.mx

Abstract. Nowadays there is a large number of tunneling projects in progress, mainly in Europe, both for roads and transport supplies. Performance prediction of tunnel boring machines (TBM) and the determination of some design parameters have become crucial, as they are critical elements in planning a project of mechanical excavation. In this paper we use the Discrete Element Method (DEM) to build models which simulate the rock cutting process under a cutting disk and measure the interaction between forces and hard rock essential in the design of TBM. The DEM is an appropriate tool for modeling geomaterials; it is assumed that a solid material can be represented by a collection of rigid particles interacting with each other in the normal and tangential directions. The particles are linked by cohesive forces which can break and simulate fracture propagation.

Keywords. Tunnel boring machine, cutting disc, lineal cutting test, cohesion.

Diseño y optimización de máquinas tuneladoras mediante la simulación del proceso de corte de roca con el método de elementos discretos

Resumen. En la actualidad existe una gran cantidad de proyectos de tunelización en proceso, principalmente en Europa, tanto para vías de comunicación como para trasporte de suministros. La predicción del desempeño de las máquinas tuneladoras (TBM) así como la determinación de algunos parámetros del diseño han llegado a ser cruciales, ya que son elementos críticos en la planificación previa de un proyecto de excavación mecánica. En este trabajo se utiliza el Método de Elementos Discretos (DEM) para construir modelos que simulan el proceso de corte de roca bajo un disco cortador. El DEM es una herramienta apropiada para para modelar geomateriales, se asume que el material sólido puede ser representado por una colección de partículas rígidas (esferas en 3D , discos en 2D) interactuando entre ellas mismas en las direcciones normal y tangencial. Las partículas estan unidas por fuerzas de cohesión que pueden romperse simulando la fractura y su propagación.

Palabras clave. Máquina tuneladora, disco cortador, prueba de corte lineal, cohesión.

1 Introduction

Predicting the performance of tunnel boring machines (TBM) is easy when the forces required in the cutting discs to fragment rock are known. However, to predict these forces is not easy because the properties of the rock mass, the disk geometry (diameter and width), the power, torque, thrust and rotational speed influence the performance of a TBM. The cutting forces also change in response to spacing between cuts and penetration. Fig. 1 shows the cutting head of a TBM. These heads may have more than 8 meters in diameter and contain more than 50 cutting discs. Fig. 3 shows a cutting disc. The forces on the cutting disc are used in the cutting head design and are the basis of many models for predicting performance of a TBM.

The models of predicting the performance of a TBM in tunneling projects can be classified as theoretical, empirical and laboratory tests. Theoretical models are based on the analysis of forces and specific energy (the energy required to excavate a unit volume of rock) and relate this analysis to the properties of rock as its compressive strength, tensile strength and shear, and finally, to machine specifications. These studies do not provide realistic values due to a

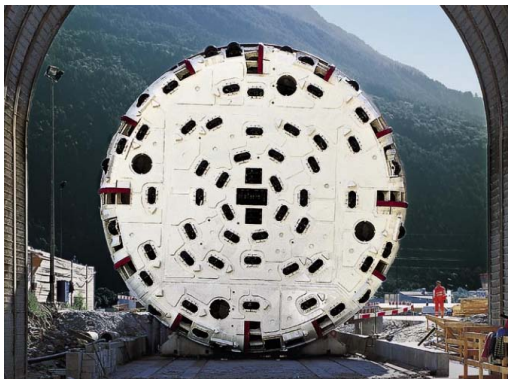

Fig. 1. Herrenknetch tunnel boring machine

complex nature of rock material. Examples of theoretical and semi-theoretical approaches can be found in [5].

Nowadays, the most reliable estimation technique is the linear cutting test (LCT). This is a test of rock cutting on large scale, where cutting forces are measured on cutters acting on large samples of rock using a linear cutting machine (LCM) [1], [3]. The LCT was developed at the Colorado School of Mines, the installation of a LCM can be observed in Fig. 2.

Fig. 2. LCM installation

The main advantage of LCT is that the design parameters such as the spacing between cuts, penetration, drive and the cutting speed can be controlled. By using load cells, all the cutting forces can be measured simultaneously as shown in Fig. 3.

The normal force is the force that has to be applied perpendicular to the rolling direction to maintain the disc at the prescribed level of penetration, therefore, it determines the thrust of a cutting machine. The rolling force is the average force required to be applied in the cutting direction to make the disc rotate to the prescribed level of penetration. The rolling force determines the power and torque requirements and is used for calculating the specific energy. The side forces are due to the

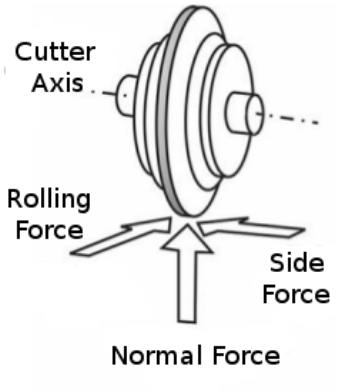

Fig. 3. Cutting disc forces

formation of a chip in the relieved side of rock while pressure is maintained on the opposite side. The side force can be used for designing the balance of the cutting head. Fig. 4 shows a theoretical analysis of the penetration of a cutting disc made in [7]. One can observe the field of stress and the resulting fractures created under the edge of the cutting disc. It is also appreciated that the radial tension forms cracks during penetration of the cutter into rock.

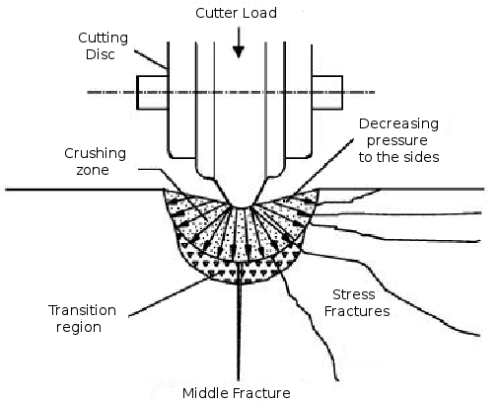

Fig. 4. Rock fracture with a single cutting disc

Fig. 5 extends this analysis to multiple disks to simulate the interaction of adjacent cuts in a TBM. In this scenario the rock under the cutter is again crushed causing radial fractures. All cracks propagate; one or more of them reach the neighbor cut causing the rock failure to produce a chip.

In this paper a simulation of the LCT using the discrete element method (DEM) is performed. The DEM is recognized as an appropriate tool

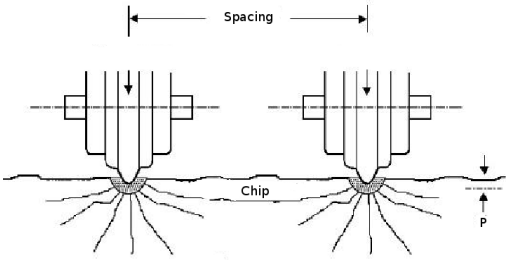

Fig. 5. Rock fracture with two cutting discs

for modeling geomaterials. The advantages of this method are used in modeling problems characterized by strong discontinuities (e.g., fracture of rock during excavation). The objective of the simulation is to measure the cutting forces acting on the disc during the process of cutting rock. These forces are essential in the design and performance prediction of a TMB. A correct simulation of the cutting forces implies an alternative to expensive laboratory testing of LCT.

2 TBM Operating Parameter Characterization

As explained in [1], the methodology used in design and characterization of the operating parameters of a TBM includes the characterization of rock and geological conditions, in this case the simulated material was granite rock. Then, the cutting tool was selected and the cutting geometry defined. A disc cutter of 432mm in diameter was used. The next step was to calculate the forces acting on the cutting discs. The DEM was used in this proposal. Finally, the specifications of the machine as thrust, torque and power based on the calculated forces on the cutters were established. The penetration rate (PR) of the TBM was estimated based on the optimum ratio spacing/penetration minimizing the specific energy. PR is defined as the excavated distance divided by the operating time of an excavation phase, while the advanced rate (AR) is the distance excavated divided by the total time including downtime for maintenance, damage to the machine, and failures in the tunnel. AR is the most important assumption made in the process of estimating the cost of any tunneling project.

2.1 Specific Cutting Energy

The specific cutting energy (SE) is the energy consumed in removing a unit material volume V [9]

$$SE = \frac{F_r \cdot l_T}{V} = \frac{F_r \cdot l_T}{p \cdot S \cdot l_T} = \frac{F_r}{p \cdot S} \tag{1}$$

where l_T is the total length traveled by the cutting disc, S is the distance between neighboring cuttings and p is the penetration. In the SE definition, only the rolling force is used because the rolling direction utilizes most of the cutting energy while the energy expended in the normal direction is negligible due to the fact that the cutting disc travels much greater distance in the tangential direction to the rock (rolling direction) than in the normal direction, although the normal force is much greater than the rolling force.

2.2 Thrust

It is necessary to know the total TBM thrust in order to calculate the power consumption. Once the optimal penetration depth is selected using the specific energy, the normal force is obtained for a cutting disk. The total thrust is estimated as

$$F_T = N_c \cdot F_N \cdot f_L \tag{2}$$

where F_N is the normal mean thrust of a disc cutter $[kN]$, N_c is the number of cutting discs and f_L is the coefficient of friction losses, usually 1.2.

2.3 Torque

Torque T on the cutting head can be estimated by considering the configuration of the TBM cutter disks based on the optimum cutting condition selected by the specific energy. Torque is the sum of the products of the distances of each disc cutter to the center of the cutterhead and the rolling force, i.e.,

$$T = \sum_{k=1}^{N} r_K F_r^k \tag{3}$$

where $r_k (k = 1, ..., N)$ are the radial distances from the center of each cutting disc to the machine center cutterhead. F_r^k denotes the rolling force of each k-th cutting disc. Without the position of the cutting discs, a good approximation can be made as shown in [2] by means of

$$T = \frac{N_C \cdot F_R \cdot D_{TBM} \cdot f_L}{4} \tag{4}$$

where F_R is the mean rolling force $[kN]$, D_{TBM} is the cutterhead diameter $[m]$, N_C is the number of cutters and f_L is the coefficient of friction losses.

2.4 Power

The cutterhead power P can be calculated considering the torque and speed in the head. Using the same approach as in [2], calculation of the power head can be performed as

$$P = 2\pi \frac{RPM}{60} T \tag{5}$$

where T is the torque of the cutting head $[kNm]$, RPM is the rotational speed $[\frac{1}{min}]$.

2.5 Net Cutting Rate

If the SE is known, then, given the power of the TBM, it is possible to calculate the net cutting rate and the penetration rate as follows:

$$ICR = \eta \frac{P}{SE} \Leftrightarrow PR \cdot \frac{\pi D^2}{4} = \eta \frac{P}{SE} \Leftrightarrow PR = \frac{4\eta P}{SE\pi D^2} \tag{6}$$

where η is the rate of energy transferred from the cutter head to the mass of the rock.

3 The Discrete Element Method

The main idea is to simulate a given material as a set of interacting particles. Cohesive bonds can exist between particles, depending on the magnitude of the bond strength. Different behaviors can be obtained and thus different materials can be simulated. It is essential to assign appropriate values of bond strength for the proper functioning of the DEM. More details on the formulation of the DEM can be found in [8] and [6].

3.1 Movement Equations

Translational and rotational movements of the particles are described by the rigid body dynamics:

$$m_i \ddot{\mathbf{u}}_i = \mathbf{F}_i \tag{7}$$

$$I_i \dot{\omega}_i = \mathbf{T}_i \tag{8}$$

where **u** is the displacement of the centroid of the element (in a fixed coordinate frame **X**); ω is the angular velocity; m is the mass of the element; I is the moment of inertia; **F** is the resulting force and **T** is the resultant moment. The vectors **F** and **T** are the sums of all forces and moments applied respectively to the i-th element due to external loads, contact interactions with neighboring spheres and other obstacles as well as forces resulting from damping the system.

The equations of motion and rotation 7, 8 are integrated in time using a centered difference scheme. The integration operator for the translational and rotational movement at the n-th step is

$$\mathbf{u}_i^{n+1} = \mathbf{u}_i^n + \dot{\mathbf{u}}_i^{n+\frac{1}{2}} \Delta t \tag{9}$$

$$\omega_i^{n+\frac{1}{2}} = \omega_i^{n-\frac{1}{2}} + \dot{\omega}_i^n \Delta t \tag{10}$$

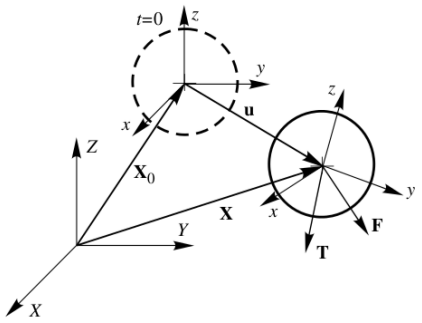

Fig. 6. Rock fracture with two cutting discs

3.2 Contact Search

The change of particle pairs in contact must be detected automatically during the process. The simplest and more expensive approach to identify particle interaction is to check each sphere against all others, which can be very inefficient because the computational time required in this approach is proportional to n^2, where n is the number of elements. In other more effective approaches, before defining the contacts, the objects are arranged spatially using an appropriate sorting algorithm. The spatial sorting determines neighbors efficiently so that any subsequent contact can be limited to those objects which are close to each other. Some algorithms of this type are the subdivision grid, binary trees, quadtrees (in 2D) and octrees (in 3D). The formulation of the contact search algorithm implemented in DEMPACK is based on spatial arrangements on quadtrees and octrees (by which time contact search is proportional to n ln n). The construction of octrees at each time step may be expensive but the information from the previous step can help us make the search for contacts more efficient. This spatial sorting is a very important HPC technique which considerably reduces the execution time of the algorithm.

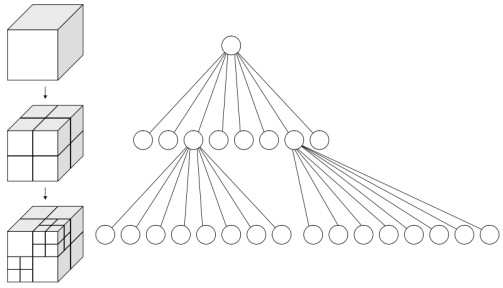

Fig. 7. Spatially ordered contact search space (octree)

3.3 Contact Force

Once pairs of contacts between particles are detected, contact forces which occur between these are calculated. The contact force **F** is decomposed into normal and tangential components:

$$\mathbf{F} = \mathbf{F}_n + \mathbf{F}_T = F_n\mathbf{n} + \mathbf{F}_T \qquad (11)$$

where **n** is the unit vector normal to the surface of the particle at the contact point (located along the line connecting the centers of the two particles) and pointing towards the outside of the particle 1 as shown in Fig. 8.

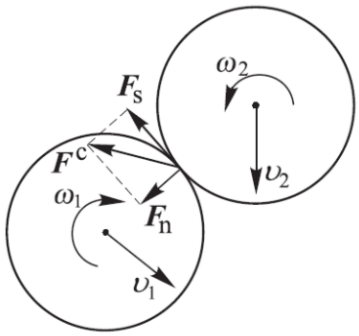

Fig. 8. Particle force decomposition

The contact forces F_n and $\mathbf{F}_T$ are obtained using a constitutive model formulated for contact between two rigid spheres (or disks in 2D). The contact interface in this formulation is characterized by normal and tangential stiffness k_n and k_T, respectively, the Coulomb friction coefficient μ and the contact damping ratio c_n, see Fig. 9. The damping is used to dissipate the kinetic energy and to reduce the oscillations of the contact forces.

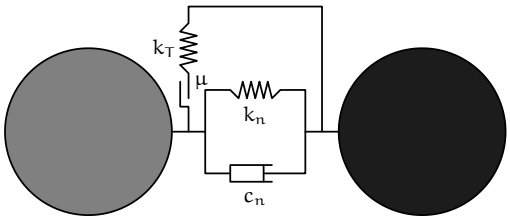

Fig. 9. Contact model interface

3.4 Elastic-Brittle Model

This model is characterized by a linear elastic behavior when cohesive bonds are active. When the cohesive strength of two particles is exceeded, a fracture occurs instantaneously in these links. When two particles are linked, the contact forces in normal and tangential directions are calculated from the linear constitutive relations:

$$\sigma = k_n u_n \qquad (12)$$

$$\tau = k_t u_t \tag{13}$$

where σ and τ are the normal and tangential contact forces, respectively; k_n and k_T are interface stiffness in normal and tangential directions, respectively; u_n and u_t are the normal and tangential relative displacements, respectively.

The cohesive bonds are broken instantaneously when the forces of the interfaces are exceeded in the tangential direction by the tangential contact force or in the normal direction by the normal contact force (traction). The failure criterion (decohesion) in 2D is written as

$$\sigma \geq R_n \tag{14}$$

$$|\tau| \geq R_t \tag{15}$$

where R_n and R_t are the resistances of the interfaces in the normal and tangential directions, respectively. In the absence of cohesion, the normal contact force can be only of compression, and the positive tangential contact force (friction force) is given by equation 17 if $\sigma < 0$ or 0 otherwise, with μ as the Coulomb friction coefficient.

$$\sigma \leq 0 \tag{16}$$

$$\tau = \mu|\sigma| \tag{17}$$

The contact laws for the normal and tangential directions of the elastic-brittle model are shown in Fig. 10 and 11, respectively. The surface failure of this model is shown in Fig. 12.

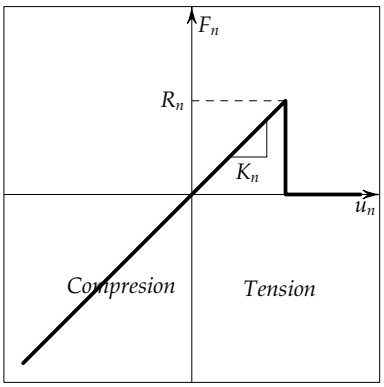

Fig. 10. Normal contact

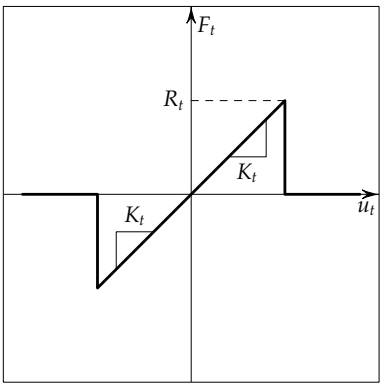

Fig. 11. Tangential contact

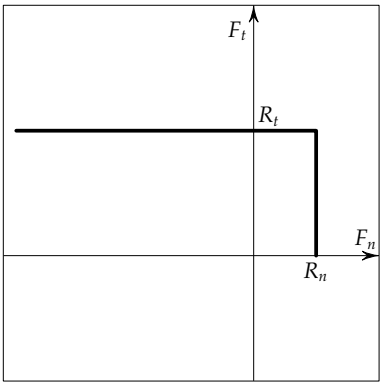

Fig. 12. Surface failure

3.5 Determination of Micromechanical Parameters

The discrete element method is a model based on micromechanical material properties. A proper choice of these parameters leads to the representation of the macroscopic properties required. In [11] detailed explanation of the conversion process between properties of the macromechanical model (the original rock sample) and the micromechanical model (the rock sample simulated by DEM) is provided. At the macroscopic level, the main parameters characterizing the rock material and its behavior in the rock cutting process are the Young's modulus E, Poisson radius ν, compressive strength σ_c and tensile strength σ_t.

This study uses the elastic-brittle constitutive model whose microparameters are contact stiffness in normal direction k_n, the contact stiffness in the tangential direction k_T, the interface tensile strength R_n, the interface tangential strength R_T and the Coulomb friction coefficient μ.

It is possible to obtain appropriate values of the microparameters combining basic laboratory simulation tests such as the unconfined compressive strength test (USC), the indirect tensile test (Brazilian test, BCS) and dimensional analysis. Details of this process can be found in [9]. The mechanical properties of rock are obtained from laboratory tests considering granite. The properties are shown in Table 1.

Table 1. Rock sample mechanical properties

Propiedad	Valor	Unidades
UCS	147.3	MPa
BCS	10.2	MPa
E	40000	MPa
ν	0.24	
ρ	2650	$\frac{kg}{m^3}$
μ	0.879	

3.6 Dimensions of the Model

The goal is to find an optimal size of the simulated rock which allows us to avoid the border effect occurring when all degrees of freedom of the base of the simulated rock sample are fixed. A larger model minimizes the edge effects but increases the computational cost having to process more particles. Edge effects can cause the normal and rolling forces to increase if the dimensions of the rock sample are too small. Other parameters to be determined are the radii of the particles and the time step size, see [8] and [6].

Through a set of LCT simulations, varying dimensions of rock sample, the radius of the elements and time step sizes, the behavior of the forces obtained were compared and the following characteristics of an optimal model (in this case) were determined: radius of the particles: 2.7mm, rock thickness: 0.05m, rock width: 0.2m, rock length: 0.4m.

Fig. 14 presents the construction of a numerical model of the LCT, Figure 15 shows damage on rock. Fig. 16 shows the cutting forces calculated by the numerical model. The peaks in these graphs are characteristic of the forces of cutting discs on brittle rock.

It is important to mention the computational cost associated to the sphere radii. Fig. 13 shows a high amount of time required for the simulations. Techniques of HPC are required. The cluster "El Insurgente" of the *Centro de Investigación en Matemáticas* was used to execute the simulations.

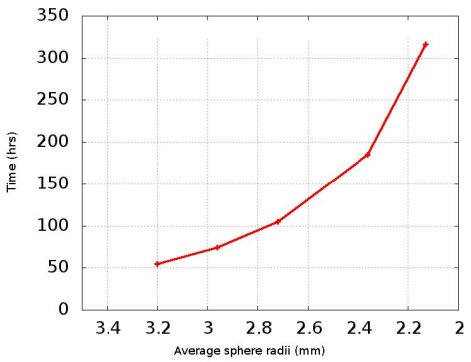

Fig. 13. Execution time depending on size (number) of spheres

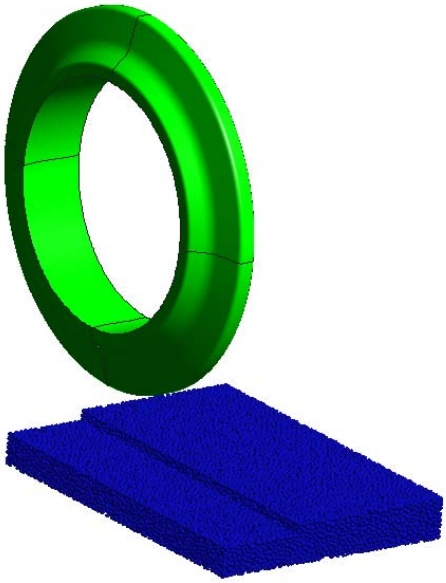

Fig. 14. DEM model of the LCT

4 Parameter Sensitivity Analysis

The influence of cutting parameters has been studied, specifically the spacing between cuts and the depth of penetration. The objective is to find an optimum ratio of spacing to penetration which minimizes the specific energy. It is necessary to perform various simulations varying these parameters.

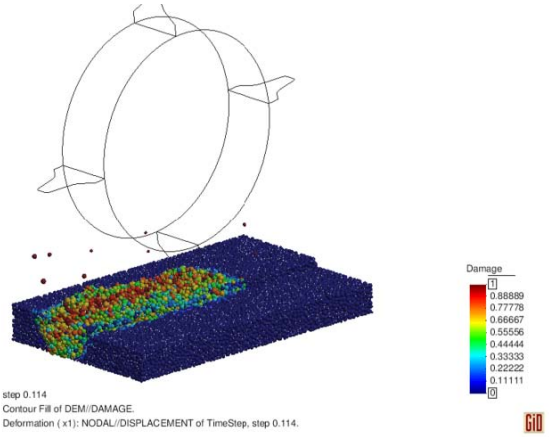

Fig. 15. Damage visualization on the simulation

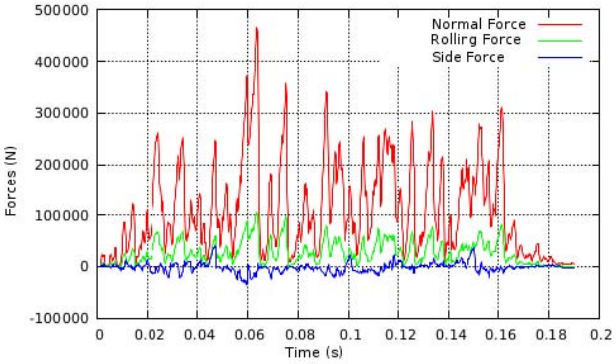

Fig. 16. Force obtained from the DEM simulation of the LCT

4.1 Penetration Depth

As the penetration increases, damage of the rock increases, which manifests itself in a higher power consumption and an increase of the normal and rolling forces [4]. Various simulations of the process of rock cutting have been performed increasing the depth of penetration from 4 mm to 12 mm. The results are shown in Fig. 15 and 16. Each of the curves is associated with a specific spacing between cuts ranging from 30 mm to 200 mm. The graphs obtained show that if the depth of penetration increases, both the rolling force and the normal force increase. The penetration depth has a major influence on the rolling force. Normal forces show a small decrease for small penetration depths (i.e., between 0.004 and 0.008 m) and an increase after the 0.008 m. This may take place because when penetration does not exceed the diameter of the spheres (in our case the mean diameter is 0.0054 m), it is difficult to capture the behavior of the normal forces.

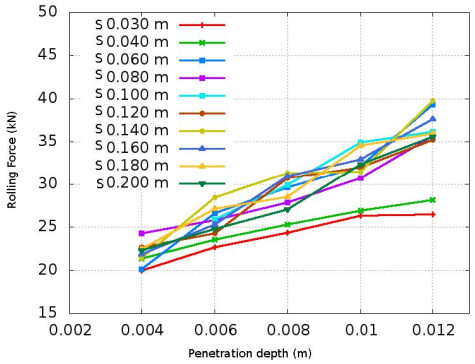

Fig. 17. Rolling forces varying the depth

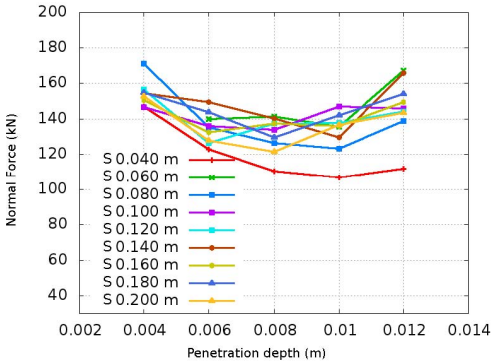

Fig. 18. Normal forces varying the depth

4.2 Spacing between Cuts

When the space between two cutters is too large, fractures develop towards the cutting line, reach the free surface and form small triangular chips. The material between the two cutting discs remains intact and forms a ridge between the two cutters. If the spacing is too small or the load is too big, cracks are developed larger but inefficient, intersect at an acute angle and form a channel between the two cutters. For optimum spacing, as illustrated in Fig. 19, fissures are propagated into the cuts ideally via a straight line approximation to their neighbors.

The size of the chips is affected by spacing. Therefore, spacing influences the machine efficiency and production. Sanio, Paul and Sikarskie [4] postulated that an increase in spacing

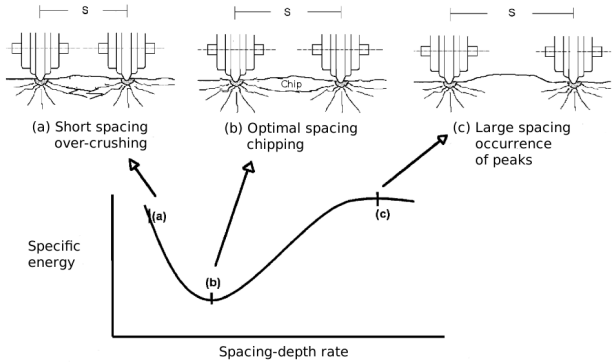

Fig. 19. Specific energy - spacing

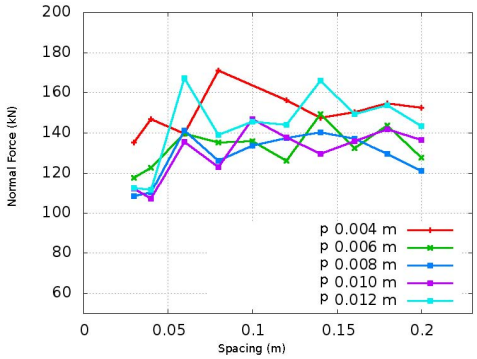

Fig. 21. Normal forces varying the spacing

should cause an increase of the normal force because rock breaks more on the side of the cutter. Too wide or too narrow spacing increase the SE. In the Ozdemir's model [10], larger spacing enables the formation of larger chips but their formation can only embark through greater penetration. We performed a set of simulations considering 10 different spacings ranging from 30 mm to 200 mm. This set of spacings was examined for each of the penetration depths previously checked. Fig. 20 and 21 show the rolling and normal forces for these cases.

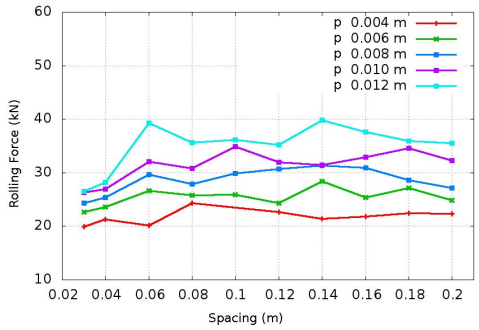

Fig. 20. Rolling forces varying the spacing

4.3 Specific Energy

Considering the SE equation and the values of the rolling forces presented in Fig. 17 and 20, the SE of the cutting process can be obtained taking into account the ratio of spacing to penetration depth. Its optimal value is the minimum SE. In Fig. 22, the SE curves obtained in simulations with DEM can be seen. x axis represents the spacing/penetration ratio and the y axis represents the energy kWh/m^3. Different curves are shown, each for a given penetration depth. Very high SE values are shown for spacing/penetration ratios below 10. As this ratio increases, the value of the SE decreases.

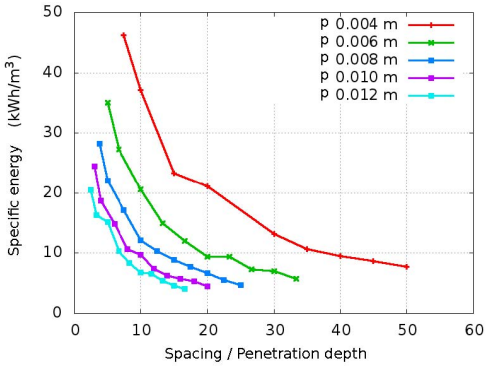

Fig. 22. Specific energy curves derived from simulation with DEM

4.4 Empirical Model CFM vs. DEM

One of the most successful empirical prediction models is the CFM (Cutting Force Method) developed at the Colorado School of Mines. Formulations for estimating the forces are based on full scale testing of cutting by different cutters in various rock types. In the CFM [10] the resultant force is obtained by

$$\frac{F_T = P^0 \Phi R T}{1 + \Psi} \tag{18}$$

where R is the radius of the cutter, T is the width or thickness of the tip of the disc, p is the

penetration per revolution, ψ is a constant for the distribution function pressure (typically from -0.2 to 0.2 decreasing at greater width of the tip), Φ is the contact angle between the rock and the cutting disc $\Phi = cos^{-1}(\frac{R-p}{R})$, and P^0 is the pressure in the crushing zone estimated from the strength of the rock and the cutting geometry. The comparison between the specific energies obtained with DEM and those obtained with CFM is shown in Fig. 23, 24, 25, 26 and 27. Big similarities between the curves of EE for penetrations greater than or equal to 0.006 m can be seen. Most significant differences occur when penetration is 0004 m.

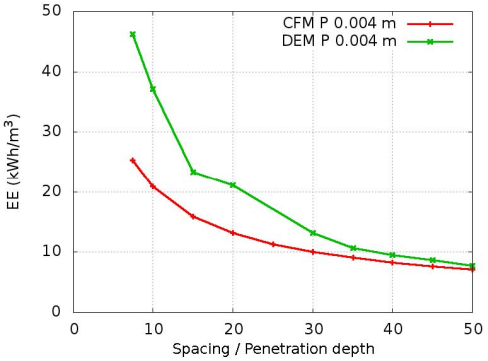

Fig. 23. Comparison of EE curves for DEM and CFM models

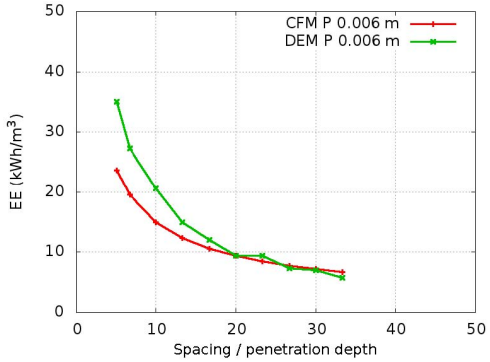

Fig. 24. Comparison of EE curves for DEM and CFM models

5 Conclusions and Future Work

Our study has shown that DEM is a highly suitable tool for geomaterial simulation. Despite having no real LCT results, comparison with CFM shows very good approximations to the forces and SE values.

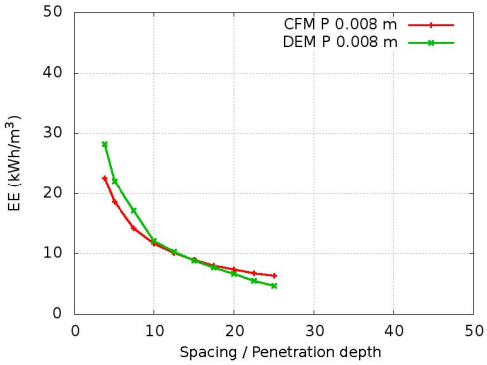

Fig. 25. Comparison of EE curves for DEM and CFM models

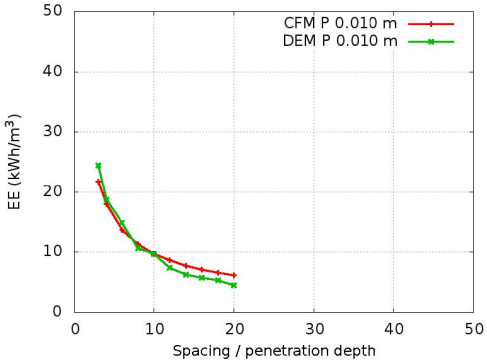

Fig. 26. Comparison of EE curves for DEM and CFM models

Although in empirical models the normal forces and the penetration of the cutter have been modeled more effectively than the rolling force and spacing, the SE is more sensitive to the last pair. The DEM accurately simulates the rolling forces on the rock cutting process and the response of the forces to variations in spacing between cuts.

DEMPACK code parallelization is of considerable interest. Implicit domain separation is performed by using an octree in searches of contacts. This makes it feasible to use distributed memory both for contact search and for the calculation of contact forces between the spheres. The use of graphics cards (GPU) should also be considered.

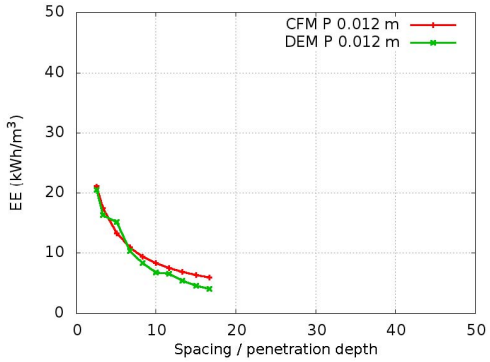

Fig. 27. Comparison of EE curves for DEM and CFM models

Acknowledgements

We would like to thank the International Center for Numerical Methods in Engineering (CIMNE) and the Center for Research in Mathematics (CIMAT), institutions which carried out this work. We are also grateful to CONACYT for financial support.

References

1. **Balci, C.** (**2009**). Correlation of rock cutting test with field performance of a TBM in highly fractured rock formation: A case study in Kozyatagi-Kadikoy metro tunnel, Turkey. *Tunneling and Underground Space Technology*, 423–435.
2. **Bilgin, N., Balci, C., Acaroglu, O., Tuncdemir, H., & Eskikaya, S.** (**1999**). The performance prediction of a TBM in tuzla-dragos sewerage tunnel. *World Tunnel Congress*, 817–822.
3. **Chang, S.** (**1995**). Performance Prediction of TBM Disc Cutting on Granitic Rock by the Linear Cutting Test. *Korea Institute of Construction Technology, Goyan-Si*.
4. **Gertsch, R., Gertsch, L., & Rostami, J.** (**2006**). Disc cutting tests in Colorado Red Granite: Implications for TBM performance prediction. *International Journal of rock mechanics and mining sciences*.
5. **Glen, F.** (**1999**). Performance Prediction for Hard-Rock Microtunneling. *North American Society for Trenchless Technology*.
6. **Medel, R.** *Predicción y optimización del desempeño de las maquinas tuneladoras mediante DEM*. Ph.D. thesis.
7. **of Mines, C. S.** (**2004**). CSM computer model for TBM performance prediction. Technical report, Earth Mechanics Institute (EMI).
8. **Oñate, E. & Rojek, J.** (**2003**). Combination of discrete element and finite element methods for dynamic analysis of geomechanics problems. *Computer methods in applied mechanics and engineering*.
9. **Rojek, J., Oñate, E., Labra, C., & Kargl, H.** (**2010**). 2D and 3D Discrete Element Simulation of Rock Cutting. *Computer methods in applied mechanics and engineering*.
10. **Rostami, J., Ozdemir, L., & Bjorn, N.** (**1995**). Comparison between CSM and NTH hard rock TBM performance prediction models. *Excavation Engineering and Earth Mechanics Institute*.
11. **Zarate, F.** (**2007**). Methodology for inverse determination of micromechanical model parameters of dem model. *TUNCONSTRUCT Deliverable*, D2.1.2.15 CIMNE.

Roberto Medel-Morales graduated from *Instituto Tecnológico de Celaya* as Computer Systems Engineer and received his M.Sc. degree in Industrial Mathematics and Computer Science from the *Centro de Investigación en Matemáticas*. He currently works at the UIF (Financial Intelligence Unit) of SHCP as an assistant manager of the statistical analysis area.

Salvador Botello-Rionda graduated from Universidad de Guanajuato as Civil Engineer and obtained his Master's degree in Engineering from the Instituo Tecnol ógico y de Estudios Superiores de Monterrey, he received his Ph.D. in the same field at the Universitat Politécnica de Catalunya . His main interests are solid mechanics and flows, applications of the Finite Element Method, multiobjective optimization and image processing. He is the author of 33 international journal papers, 8 national journal papers, 19 books and 15 book chapters. He is a member of the National System of Researches of Mexico, Level II. Also, he has been an editor of 6 conference proceedings.

Article received on 19/02/2013; accepted on 11/08/2013.